NUCLEAR REACTIONS IN DENSE STELLAR MATTER*

D.G. YAKOVLEV

A.F. Ioffe Institute of Physics and Technology
194021, St.Petersburg, Russia

(Received August 28, 1993)

Five possible regimes of nonresonant nuclear fusion reactions in dense stellar matter are briefly reviewed. They are: classical thermonuclear (weak screening) regime; thermonuclear strong screening burning regime; pycnonuclear (zero-temperature) regime; thermally enhanced pycnonuclear burning; and the regime intermediate between the thermo- and pycno-nuclear ones.

PACS numbers: 97.10. Cv

1. Introduction

Nuclear reactions are important during all stages of stellar evolution. This work deals with nonresonant nuclear fusion reactions in dense stellar matter when colliding nuclei, 1 and 2, form a compound nucleus c which undergoes further transformations. Not too high temperatures $T \lesssim (3-5) \times 10^9$ K will be considered when nuclei are not dissolved and penetrate a substantial Coulomb barrier in nuclear reactions. In all cases important for applications one can restrict oneself by densities $\rho \lesssim 10^{11}$ g cm^{-3}.

The rate of nuclear burning depends strongly on chemical composition of matter, as well as on temperature and density (Sect. 2). Five different nuclear burning regimes are possible in dense matter. They are reviewed briefly in Sects 3–7. The results are summarized in Sect. 8.

---

* Presented at the XXIII Mazurian Lakes Summer School on Nuclear Physics, Piaski, Poland, August 18–28, 1993.

2. Properties of dense stellar matter

In the density-temperature domain of study (Fig. 1) stellar matter consists of almost free electrons and of atoms which are fully ionized either by high T or by high electron pressure. Let n_e be number density of electrons and n_ν be number density of ion species $\nu = 1, \ldots, s$ (with atomic number A_ν and charge number Z_ν). For $s > 1$ we have a *multicomponent plasma* of ions, while for $s = 1$ we have a *one-component plasma* (OCP) of ions. In the case of OCP the index ν will be often omitted.

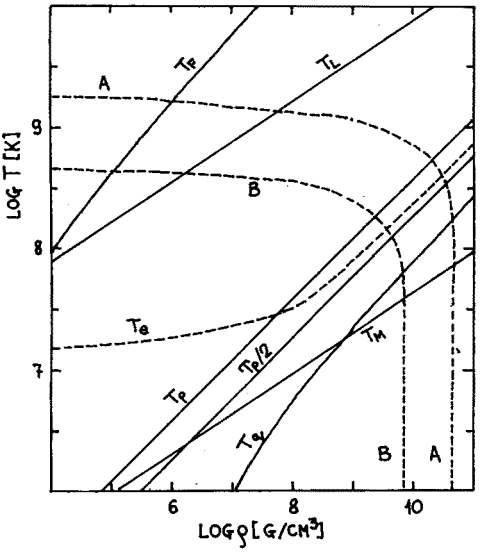

Fig. 1. Density-temperature diagram for a carbon plasma. T_l is the temperature below which the ions form Coulomb liquid; T_m is the melting temperature; T_p is the ion plasma temperature; T_e is the temperature below which the electron screening is strong ($E_e > 2$); T_q is the temperature below which the reaction rate is temperature independent. Lines A and B correspond to burning of carbon in $t = 1$ s, and 10^9 yrs, respectively.

The electron degeneracy temperature (see Fig. 1) is given by $T_F = T_0(\sqrt{1+x^2} - 1)$, where $T_0 = m_e c^2 \approx 5.930 \times 10^9$ K, m_e is the electron mass, x is the electron "relativistic parameter",

$$x = \frac{p_F}{m_e c} \approx 1.009 \left(\frac{\rho_6}{\mu_e}\right)^{1/3}, \qquad p_F = \hbar(3\pi^2 n_e)^{1/3}, \tag{1}$$

p_F is the electron Fermi momentum, ρ_6 is density in units of 10^6 g cm^{-3}, and μ_e is the mean molecular weight per electron ($\mu_e = A/Z$ for OCP). Here and in what follows the Boltzmann constant is put equal to $k_B = 1$.

Ion state is defined by the ion-coupling parameter

$$\Gamma_\nu = \frac{Z_\nu^2 e^2}{a_\nu k_B T} \approx 0.2275 \frac{Z_\nu^{5/3}}{T_8} \left(\frac{\rho_6}{\mu_e}\right)^{1/3}, \qquad (2)$$

where $a_\nu = \left(3Z_\nu/(4\pi n_e)\right)^{1/3}$ is the radius of ion sphere (which contains Z_ν electrons whose charge compensates the ion charge), and $T_8 = T/(10^8\,\mathrm{K})$.

At sufficiently high temperatures the ions form a classical Boltzmann gas. With decreasing T, the gas gradually (without a phase transition) becomes a Coulomb liquid, and then (with a phase transition) a crystal. The gaseous regime of an OCP occurs [1] for $\Gamma \ll 1$ ($T \gg T_l$, Fig. 1). The melting of a classical OCP takes place [2] at $\Gamma \approx 172$ ($T = T_m$).

At low T the quantum effects in the ion motion (zero-point ion vibrations) become important. These effects are especially pronounced if $T \ll T_p$, where $T_p = \hbar\omega_p$, and ω_p is the ion plasma frequency. For an OCP, one has

$$T_p \approx 7.832 \times 10^6 \left(\frac{\rho_6}{\mu_e^2}\right)^{1/2} \mathrm{K}, \quad \omega_p^2 = \frac{4\pi Z^2 e^2 n_i}{m_i}, \qquad (3)$$

where n_i is the number density of ions, and m_i is the ion mass. The amplitude of zero-point ion vibrations is commonly much smaller than typical inter-ion distance, a. With increasing density, this amplitude becomes larger (with respect to a), and at large ρ zero-point vibrations can prevent crystallization. In the density range of study, this effect is important for H and He only [3, 4]. The $\rho - T$ diagrams for ion mixtures are discussed, for instance, in [5], and in the references therein.

3. Classical theory of thermonuclear reactions

According to the classical theory [6] the rate R_0 ($\mathrm{cm}^{-3}\ \mathrm{s}^{-1}$) of a thermonuclear reaction ($Z_1 + Z_2 \to Z_c$) is

$$R_0 = \frac{n_1 n_2}{1+\delta} \langle v\sigma \rangle, \qquad (4)$$

where n_1 and n_2 are number densities of reacting nuclei, $\delta = 1$ if these nuclei are equal and $\delta = 0$ otherwise, $v = |v_1 - v_2|$ is a relative velocity of the nuclei, σ is the reaction cross section, and brackets denote averaging of $v\sigma$ over relative velocities with Maxwellian distribution function.

The reaction cross section is commonly written as

$$\sigma = \frac{SP}{\varepsilon}, \quad P = \exp\left(-\sqrt{\frac{\varepsilon_G}{\varepsilon}}\right), \quad \varepsilon_G = \frac{M}{2}\left(\frac{2\pi e^2 Z_1 Z_2}{\hbar}\right)^2. \qquad (5)$$

In this case, $\varepsilon = Mv^2/2$ is a relative collision energy, M is the reduced mass, P is the Coulomb barrier penetration probability, and $S(\varepsilon)$ is the astrophysical factor which describes the reaction efficiency after the barrier penetration. For a nonresonant reaction, S is a smooth function of ε and the averaging $\langle v\sigma\rangle$ is easily performed by the "saddle-point" method, yielding

$$\langle v\sigma\rangle = \sqrt{\frac{32\varepsilon_{pk}}{3M}}\frac{S(\varepsilon_{pk})}{T}\mathrm{e}^{-\tau}, \quad \tau \approx 9.1535\left(\frac{A_1A_2Z_1^2Z_2^2}{(A_1+A_2)T_8}\right)^{1/3}, \qquad (6)$$

where $\tau = 3(\varepsilon_G/4T)^{1/3}$. In a stellar matter one commonly has $\tau \gg 1$. In this case, the reaction is strongly suppressed by the Coulomb barrier. The main contribution to (6) comes from collisions with suprathermal energies ε which lie in a relatively narrow interval of width $\Delta\varepsilon \approx \sqrt{\varepsilon_{pk}T}$ in the vicinity of the Gamov-peak energy $\varepsilon_{pk} = \tau T/3$. A typical tunneling length at these energies is $r_{tn} \approx Z_1Z_2e^2/\varepsilon_{pk}$. With decreasing T, the parameter τ grows as $T^{-1/3}$. The reaction rate becomes lower, Gamov peak energy is more suprathermal ($\varepsilon_{pk}/T \approx \tau/3$), and the tunneling length larger.

As will be shown in Sect. 4, the classical thermonuclear burning regime operates at $T \gtrsim T_l$.

4. Plasma screening in thermonuclear reactions

4.1. General formula

In dense stellar matter the effects of *plasma screening* in thermonuclear reactions become important. These are the effects of surrounding plasma particles (electrons and ions) onto the reaction of colliding nuclei. The plasma electrons and ions affect the collisions of the reacting nuclei 1 and 2 in different ways. Let $v_{pk} = \sqrt{2\varepsilon_{pk}/M}$ be a typical velocity of the reacting nuclei, v_e a typical velocity of plasma electrons, and v_i a typical (thermal) velocity of plasma ions.

The plasma electrons are much faster than the colliding nuclei ($v_e \gg v_{pk}$). Then one can assume that the electrons form a continuous background that is weakly but almost instantly polarized by the ions. On the contrary, the plasma ions are commonly much slower than the reacting nuclei ($v_i \ll v_{pk}$). Accordingly, one should initially calculate the reaction probability for fixed positions of the plasma ions and then average over these positions.

The screening can be described by the factor E defined as

$$E = \frac{R}{R_0}, \quad R = \frac{n_1n_2}{1+\delta}\overline{\langle v\sigma\rangle}, \qquad (7)$$

where R is the actual reaction rate, and R_0 is the classical rate (4). Upper line denotes additional averaging over positions of the plasma ions. In the thermonuclear regime (quantum effects in ion motion are ignored), the averaging can be performed with the classical Gibbs distribution of ions. The screening effects increase the reaction rate, and E is called *the enhancement factor* of the thermonuclear reaction ($E > 1$).

Explicit calculation of E is difficult but one important case is well known. Let V be interaction potential of the reacting nuclei in a plasma. It can be written as $V = (Z_1 Z_2 e^2/r) + \Phi$, where $\Phi(r|r_c, r_3, \ldots, r_N)$ is the plasma screening term which depends on a relative distance between the reacting nuclei $r = r_2 - r_1$, on their center of mass r_c, and on positions of neighbouring plasma ions $r_3, \ldots, r_N$. The positions $r_c, r_3, \ldots, r_N$ are fixed for each reaction event, while R is the average over the events. Let $l \sim a$ be a typical length scale of Φ as a function of r, and let $l \gg r_{tn}$. In the latter case, $\Phi(r)$ may be regarded as constant, $\Phi(0)$, for a tunneling event, and the plasma screening affects only the probability for the colliding nuclei to approach the tunneling region $r \lesssim r_{tn}$. Then one obtains:

$$E = \overline{\exp\left(-\frac{\Phi(0)}{T}\right)} = \lim_{r\to 0} \exp\left(\frac{Z_1 Z_2 e^2}{Tr}\right) g(r) = \exp(H(0)). \qquad (8)$$

In this case,

$$g(r) = \exp\left(-\frac{Z_1 Z_2 e^2}{Tr} + H(r)\right) \qquad (9)$$

is the radial-pair distribution function for ions 1 and 2. It is proportional to the probability for these ions to be at a distance r and it is normalized as $g \to 1$ as $r \to \infty$. $H(r)$ is the so called *mean field potential* created by surrounding plasma particles. $g(r)$ and $H(r)$ have been studied intensively by Monte Carlo method and various methods of the theory of liquids; see, *e.g.*, [7 – 11], and the references therein.

Using standard thermodynamic relationships (see, *e.g.*, [5]), Eq. (8) can be rewritten in the Boltzmann form,

$$E = \exp\left(-\frac{\Delta\mu^{\mathrm{C}}}{T}\right), \quad \Delta\mu^{\mathrm{C}} \equiv \mu_c^{\mathrm{C}} - \mu_1^{\mathrm{C}} - \mu_2^{\mathrm{C}}, \qquad (10)$$

where $\mu_\nu^{\mathrm{C}} = \partial F^{\mathrm{C}}/\partial N_\nu$ is the Coulomb part of the chemical potential of ions of species ν ($\nu = c$ refers to a compound nucleus, $Z_c = Z_1 + Z_2$) determined by the Coulomb component of the Helmholtz free energy F^{C}. Eqs (8) and (10) represent the basis of the screening theory [12 – 14].

The main condition of validity for (8) and (10) is $r_{tn} \ll l$. For estimations, one can take an unscreened tunneling length r_{tn} and set $l \sim a$, the ion

sphere radius. Then, for a nuclear reaction in OCP, the inequality $r_{tn} \ll l$ is equivalent to $T \gg T_p$ (Fig. 1). The inequality can also be rewritten as $\varepsilon_{pk} \gg Z^2e^2/a$ or as $\tau \gg \Gamma$.

4.2. Weak screening

If $T \gg T_l$ the ions constitute almost perfect Boltzmann gas, and $g(r)$ in (9) is given by the Debye–Hückel theory, $g(r) = \exp(-V(r)/T)$, where $V(r) = Z_1 Z_2 e^2 \exp(-r/r_D)/r$ and r_D is the screening length of an electric charge in a plasma. This immediately yields $H(0) = Z_1 Z_2 e^2/(r_D T)$. Under these conditions, the screening is commonly week, $H(0) \ll 1$, $(E-1) \ll 1$, and the classical theory of thermonuclear burning (Sect. 3) is valid.

For example, consider a hydrogen-helium plasma (with hydrogen abundance $X = 0.7$, by mass) in the solar center, $T = 1.5 \times 10^7$ K, $\rho = 150$ g cm^{-3}. The plasma is nondegenerate, and one can treat r_D as the classical Debye radius. Then for the leading reaction (^{1}H(p,e$^+$)^{2}H) of hydrogen burning in the proton cycle we have $E \approx 1.055$. The screening enhances thermonuclear burning by about 5%.

4.3. Ion and electron screening

If $T_p \ll T \lesssim T_l$ the electron gas is commonly strongly degenerate and constitutes almost uniform background. Then in Eq. (10) one can put $\mu_\nu^C = \mu_\nu^U + \mu_\nu^P$, where μ_ν^U is the Coulomb chemical potential calculated in the uniform electron background approximation, and μ_ν^P is a small correction produced by weak polarization of the electron gas. Accordingly,

$$E = E_i E_e\,,\quad E_{i,e} = \exp(H_{i,e})\,,\quad H_i = -\frac{\Delta\mu^U}{T}\,,\quad H_e = -\frac{\Delta\mu^P}{T}\,. \qquad (11)$$

E_i will be called the *ion screening* factor, while E_e will be called the *electron screening* factor. Commonly the ion screening dominates, $H_i \gg H_e$.

4.4. Strong ion screening

The problem reduces to calculating μ_ν^U in a multicomponent ion plasma. Luckily, according to extensive studies [9], strongly coupled Coulomb ion mixtures obey additive rule. This means that, with very high accuracy, one has: $\mu_\nu^U/T = f(\Gamma_\nu)$, where $f(\Gamma)$ is a universal function of Γ which can be determined from the studies of OCP, *e.g.*, [15, 9 – 11]. A convenient fitting expression was proposed by DeWitt [15]. Being applied to the Monte Carlo data of [11] at $1 \le \Gamma \lesssim 170$, this expression yields

$$f(\Gamma) = A\Gamma + 4B\Gamma^{1/4} - 4C\Gamma^{-1/4} + D\log\Gamma + F\,, \qquad (12)$$

where $A = -0.897744$, $B = 0.95043$, $C = 0.18956$, $D = -0.81487$, $F = -2.5820$. When $\Gamma \gg 1$ the result $f \approx A\Gamma$ is very close to that given by the simple ion-sphere model [12], $f^{IS} = -0.9\Gamma$.

Eqs (11) and (12) yield $H_i = f(\Gamma_1) + f(\Gamma_2) - f(\Gamma_c)$ which allows one to calculate easily E_i for $T_p \ll T \lesssim T_l$. When temperature is much below T_l ($\Gamma \gg 1$) the exponent factor H_i is nearly linear in Γ ($H_i \approx A(2-2^{5/3})\Gamma \approx 1.055\Gamma$ for $Z_1 = Z_2$), and the ion screening becomes very strong. For instance, $E_i = 6.4 \times 10^{46}$ for a reaction with equal nuclei in OCP at $\Gamma = 100$.

4.5. Strong electron screening

Calculations of E_e for $T_p \ll T \lesssim T_l$ were performed in [5] (also see [5] for a critical analysis of preceding works). We will not present the numerical results [5] but give an order of magnitude estimate for an equal-charge reaction in OCP: $H_e \sim H_i(ak_{TF})^2$, where a is the ion-sphere radius of the reacting nuclei, $k_{TF} = \sqrt{\omega_{pe}}/v_F$ is an inverse length of screening of an electric charge by strongly degenerate electrons, and v_F is the electron Fermi velocity. The factor $(ak_{TF})^2 \sim 4.7Z^{2/3}e^2/(\hbar v_F) \sim 0.03Z^{2/3}\sqrt{1+x^2}/x$ is generally small and reflects weak compressibility of the electron gas. Accordingly, the electron screening is commonly much weaker than the ion one and of less astrophysical importance. However, the electron screening can be strong by itself. The temperature T_e in Fig. 1 corresponds to $E_e = 2$ for the carbon burning and restricts the domain of strong electron screening, $T \lesssim T_e$. With decreasing ρ, the parameter $(ak_{TF})^2$ becomes larger and the electron screening gets more important as compared to the ion screening. For $\rho \sim AZ$ g cm^{-3}, the electron screening becomes comparable with the ion one, $H_e \sim H_i$, but the above approaches to the screening problem fail at these low densities (ionization becomes incomplete, electrons are strongly non-ideal).

5. Pycnonuclear reaction regime

Pycnonuclear reaction regime operates even at $T = 0$. In this regime, the Coulomb tunneling takes place due to zero point vibrations of nuclei in their lattice cites. Basic theoretical aspects of pycnonclear reactions were considered in the fundamental work [16]. The reaction is controlled by a very weak tunneling of the nuclei. Each nucleus can actually interact with the closest neighbors only: the tunneling probability of more distant nuclei is negligible. The pycnonuclear reaction rate R_p in a bcc lattice of OCP is given by $R_p = (8n_i)Q/2$ since each nucleus is surrounded by 8 closest neighbors. Here Q is the reaction frequency (s^{-1}) for a pair of nuclei (1 and 2). The tunneling is most efficient if the center of mass of the reacting

nuclei is fixed at its equilibrium position. The most sensitive problem is the calculation of the interaction potential $V(r)$ of nuclei 1 and 2 including possible response of the neighbors. Salpeter and Van Horn [16] calculated R_p in two approximations. In the *static* approximation, the neighboring nuclei are fixed at their lattice sites. In the *relaxed* approximation, they are allowed to adjust themselves fully to displacements of the reacting nuclei. In any case, $V(r)$ appears to be of oscillatory type for small displacements of nuclei 1 and 2 from the lattice sites, and $V(r)$ tends to the bare Coulomb potential when $r \ll a$. The oscillator frequency ω_0 is about ω_p (see (3)), and typical zero-point displacements are $r_0 \sim \sqrt{\hbar/(m_i\omega_p)}$.

Recently, the calculations [16] have been extended [17] using somewhat more detailed interaction potentials $V(r)$. In Ref. [18], the pycnonuclear reaction rates have been calculated with some mean directionally-averaged potential $V(r)$ (for OCP and binary ionic mixtures). These results have been extended further in [19]. For OCP, the results [17 – 19] are close to [16]. For instance, according to [17]

$$R_p = 10^{55} C S A Z^4 \rho_8 \lambda^{7/4} \exp(-\gamma)\ \mathrm{cm^{-3}s^{-1}}, \tag{13}$$

$$\lambda = \left(\frac{n_i}{2}\right)^{1/3} \frac{\hbar^2}{Z^2 e^2 m_i} \approx 0.09032 \frac{\rho_8^{1/3}}{Z^2 A^{4/3}}, \tag{14}$$

where S is the astrophysical factor measured in MeV bn, $\gamma = \alpha_1/\sqrt{\lambda}$. In the static approximation, one has $C = 5.8$, $\alpha_1 = 2.639$, while in the relaxed approximation $C = 9.09$, $\alpha_1 = 2.516$. The main quantity is the exponent argument γ which determines the tunneling probability. Note that γ can be rewritten as $\gamma = \beta m_i \omega_p a^2/\hbar = 3\beta Z^2 e^2/(aT_p)$, with $\beta = (8\pi/81)^{1/6}\alpha_1$. Thus, γ is similar to the ion-coupling parameter (2), where temperature T is replaced by the "quantum temperature" T_p.

For $\rho = (10^9 - 10^{10})$ g cm^{-3}, the pycnonuclear carbon burning rate in the relaxed approximation is (2-3) orders of magnitude larger than in the static approximation. Kinetic energy of responding neighboring ions in the relaxed approximation can be treated [17] in terms of renormalization of reduced mass of the colliding nuclei. An allowance for this effect [17] shifts the reaction rate R_p calculated in the relaxed approximation to that in the static approximation.

The static approximation would be exact if $\omega_p t_{tn} \ll 1$, while the relaxed approximation would be exact if $\omega_p t_{tn} \gg 1$. Here t_{tn} is the tunneling time, and ω_p^{-1} is a typical response time of the neighbouring nuclei. A simple WKB estimate of t_{tn} yields $\omega_p t_{tn} \sim 1$ (contrary to the conclusion of [17]). Thus, actually the ion response is neither static nor relaxed but dynamic.

As shown in [17], the pycnonuclear burning depends on the lattice type. One cannot exclude that nuclei form the fcc lattice rather than bcc. The

binding energy of a nucleus in a fcc lattice is lower, but the difference (about $10^3 Z^{5/3}(\rho_6/\mu_e)^{1/3}$ K in temperature units) is negligible according to astrophysical standards. For $\rho \sim (10^9 - 10^{10})$ g cm^{-3}, the pycnonuclear carbon burning rate in fcc lattice is (5-8) orders of magnitude larger [17] than in bcc. The difference comes mainly from different tunneling probabilities which are sensitive to closest distances between the nuclei in a lattice and to the parameters of the interaction potential $V(\mathrm{r})$. The closest distances and the potential parameters can vary noticeably for ionic mixtures [19] and/or in the presence of lattice imperfections [16]. All these effects introduce additional uncertainty into our knowledge of actual values of R_p.

The pycnonuclear burning does not depend on T but increases with density because zero-point vibrations become more important at higher ρ. As will be shown in Sect. 6 the burning remains temperature independent for $T \lesssim T_p/\log(T_l/T_p)$.

6. Thermal enhancement of pycnonuclear burning

When T increases from $T = 0$, the reaction rate R becomes temperature dependent. If T is not very large, it is convenient to introduce the *thermal enhancement factor*,

$$E_p = \frac{R}{R_p}, \tag{15}$$

where R is the actual reaction rate, and R_p is the pycnonuclear rate. The temperature dependence of R at $T \lesssim T_p$ was considered in [16]. The main effect is concerned with thermal increase of energies of the reacting nuclei. The effect is especially simple when energy ε of relative motion of the nuclei is much smaller than the Coulomb energy, $U_c \sim Z^2 e^2/a$. In this case the barrier penetration probability is $P(\varepsilon) \approx \exp(-h)\exp\left((\varepsilon/\omega_0)\log(U_c/\varepsilon)\right)$, where ω_0 is the fundamental oscillator frequency (Sect. 5). The probability increases rapidly with ε while the energy distribution of the nuclei, $f = \exp(-\varepsilon/T)$, is a rapidly decreasing function. The reaction rate is expressed through the sum of products fP over various quantum states of the reacting nuclei. The competition of two factors, f and P, produces a peak at energy ε_{pk} similar to the Gamov peak in the thermonuclear burning (Sect. 3). The peak position and the reaction rate can be evaluated by the same "saddle-point" method. According to [16], $\varepsilon_{pk} \sim \hbar\omega_p + U_c \exp(-\zeta U_c/T)$, where $\zeta \sim 1$ is a numerical factor. Thus, the thermal enhancement becomes important for $T \gtrsim T_p/\log(T_l/T_p)$, when ε_{pk} grows rapidly with T and becomes much larger than the zero-point energy. For $T \approx T_p/2$, the peak energy becomes comparable to the Coulomb energy U_c, and then the thermal enhancement regime is over. Note that neighbouring ions remain mainly in their ground state over all the enhancement regime.

Thus, the $T = 0$ pycnonuclear regime discussed in Sect. 5 operates at $T \lesssim T_p/\log(T_l/T_p)$. The regime of thermal enhancement of pycnonuclear burning is valid in a narrow temperature interval, $T_p/\log(T_l/T_p) \lesssim T \lesssim T_p/2$. The enhancement factor (15) for the latter regime was calculated [16] in the relaxed and static approximations. The temperature dependence of E_p can be approximately described as $E_p \sim \exp\left((U_c/\hbar\omega_0)\exp(-\hbar\omega_0/T)\right)$. When density grows, the T_l/T_p-ratio becomes lower, and the temperature interval of the thermal enhancement regime becomes narrower. Accordingly, the regime is less pronounced. If, for instance, $T = T_p/2$ one has $E_p \sim (10^7 - 10^8)$ (depending on the approximation used) for the carbon burning at $\rho = 10^9$ g cm^{-3}, and $E_p \sim 10^5$ for $\rho = 10^{10}$ g cm^{-3}.

7. Intermediate thermo/pycno-nuclear burning regime

This regime occurs in the temperature range $T_p/2 \lesssim T \lesssim T_p$. It is most difficult for theoretical description. The peak energies of the reacting nuclei are comparable to the Coulomb energy, Z^2e^2/a. The reacting nuclei are neither tightly bound to their equilibrium positions nor entirely free. The interaction potential of these nuclei $V(\mathbf{r})$ depends on the positions of neighboring ions. The regime is intermediate (between quantum and classical domains) for the neighboring ions as well: the ions occupy several low energy states.

Many authors approach this regime from high-temperature domain, introducing the screening factors $E = R/R_0$ and calculating the tunneling probability in the mean-field approximation (see [20,18], and the references therein). In this approximation, the interaction potential is taken in the form $V = Z_1 Z_2 e^2 r^{-1} - H(r)T$, where $H(r)$ is the mean-field potential, see (9). Note that in a series of works [20, 18] the r^4 term in the small-r expansion of $H(r)$ is calculated inaccurately [21]. This, however, cannot introduce an essential error into E. A comparison of the reaction rates calculated in the mean-field approximation [18] with those based on the screening factors of Sect. 4 shows that the simple screening approach of Sect. 4 becomes invalid at $T \lesssim T_p$. In the range of $T_p/2 \lesssim T \lesssim T_p$ the mean-field results give some interpolation (Fig. 2) between the simple screening regime (Sect. 4) and thermally enhanced pycnonuclear regime (Sect. 6). The accuracy of this interpolation is not very well known. Actually, the reaction rates can be strongly affected [22, 23] by fluctuations of the interparticle potential $V(\mathbf{r})$ introduced by neighbouring ions. In a rigorous theory, one should determine the barrier penetration factor in a random potential and then average this factor over an ensemble of fluctuations. This rigorous approach has not yet been realized (although some simplified attempts have been undertaken [24]).

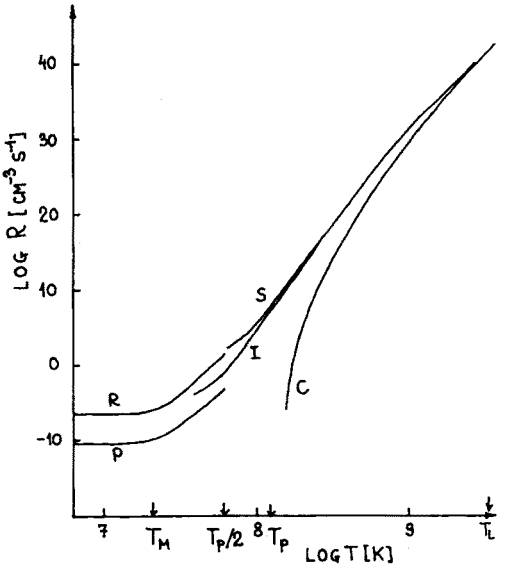

Fig. 2. Temperature dependence of the carbon burning reaction rate in carbon matter at $\rho = 10^9$ g cm^{-3}. C is the classical thermonuclear reaction rate; S is the rate with the strong screening factor of Sect. 4; I is the same with the screening factor [18] calculated in the mean-field approximation. Curves R and P show the pycnonuclear reaction rates in the relaxed and static approximations, respectively. The $T = 0$ results are taken from [17] (bcc lattice), while the thermal enhancement factors are from [16].

8. Summary

Non-resonant nuclear reactions in dense stellar matter can proceed in five regimes (Fig. 1) depending on temperature, density, and chemical composition of matter. The classical thermonuclear burning (Sect. 3) occurs at $T \gg T_l$. The thermonuclear regime with strong screening (Sect. 4) takes place at $T_p \ll T \lesssim T_l$. The temperature independent pycnonyclear regime (Sect. 5) is realized at $T \lesssim T_p/\log(T_l/T_p)$. The regime of thermal enhancement of pycnonuclear burning (Sect. 6) operates at $T_p/\log(T_l/T_p) \lesssim T \lesssim T_p/2$. Finally, the intermediate thermo/pycno-nuclear burning (Sect. 7) occurs at $T_p/2 \lesssim T \lesssim T_p$. Fig. 2 shows the temperature dependence of the carbon burning rate for $\rho = 10^9$ g cm^{-3}. Different burning regimes are quite visible.

The many-body effects in dense matter greatly amplify the reaction rates at $T \lesssim T_l$ as compared to the classical thermonuclear rates. These effects are especially pronounced in the pycnonuclear regime: they allow the nuclei to react even at $T = 0$. Curves A and B in Fig. 1 show the lines in the $\rho - T$ plane where the mean burning time of carbon matter $t = n_i/R$

equals 1 s and 10^9 yrs, respectively. The pycnonyclear burning of carbon is seen to be most essential at $\rho \gtrsim 10^{10}$ g cm^{-3}.

The physical nature of nuclear burning in all 5 reaction regimes is understood quite adequately. The existing theoretical description of nuclear reactions is most reliable for $T \gtrsim T_p$ (classical thermonuclear and strong screening thermonuclear burning). For lower temperatures, the results (Secs 5–7) are not so very certain.

This work has been supported in part by KBN grant No. 2-1244-91-01 and by ESO C&EE Programme grant No. A-01-068.

REFERENCES

[1] S.G. Brush, H.L. Sahlin, E. Teller, *J. Chem. Phys.* **45**, 2102 (1966).
[2] H. Nagara, Y. Nagata, T. Nakamura, *Phys. Rev.* **A36**, 1859 (1987).
[3] R. Mochkovitch, J.-P. Hansen, *Phys. Lett.* **A73**, 35 (1979).
[4] D.M. Ceperley, B.J. Alder, *Phys. Rev. Lett.* **45**, 566 (1980).
[5] D.G. Yakovlev, D.A. Shalybkov, *Sov. Sci. Rev.*, R.A. Syunyaev ed., **E7**, 313 (1989).
[6] M. Schwarzschild, *Structure and Evolution of the Stars*, Princeton University Press, Princeton, 1958.
[7] J.-P. Hansen, *Phys. Rev.* **A8**, 3096 (1973).
[8] E.L. Pollock, J.-P. Hansen, *Phys. Rev.* **A8**, 3110 (1973).
[9] J.-P. Hansen, G.M. Torrie, P. Vieillefosse, *Phys. Rev.* **A16**, 2153 (1977).
[10] W.L. Slattery, G.D. Doolen, H.E. DeWitt, *Phys. Rev.* **A21**, 2087 (1980).
[11] W.L. Slattery, G.D. Doolen, H.E. DeWitt, *Phys. Rev.* **A26**, 2255 (1982).
[12] E.E. Salpeter, *Australian J. Phys.* **7**, 353 (1954).
[13] H.E. DeWitt, H.C. Graboske, M.S. Cooper, *Ap. J.* **181**, 439 (1973).
[14] H.C. Graboske, H.E. DeWitt, A.S. Grossman, M.S. Cooper, *Ap. J.* **181**, 457 (1973).
[15] H.E. DeWitt, *Phys. Rev.* **A14**, 1290 (1976).
[16] E.E. Salpeter, H.M. Van Horn, *Ap. J.* **155**, 183 (1969).
[17] S. Schramm, S.E. Koonin, *Ap. J.* **365**, 296 (1990); *Ap. J.* **377**, 343 (1991).
[18] S. Ogata, H. Iyetomi, S. Ichimaru, *Ap. J.* **372**, 259 (1991).
[19] S. Ichimaru, S. Ogata, H.M. Van Horn, *Ap. J.*, **401**, L35 (1992).
[20] S. Ichimaru, *Rev. Mod. Phys.* **65**, 255 (1993).
[21] Y. Rosenfeld, *Phys. Rev* **A46**, 1059 (1992).
[22] B. Jancovici, *J. Stat. Phys.* **17**, 357 (1977).
[23] A. Alastuey, B. Jancovici, *Ap. J.* **226**, 1034 (1978).
[24] M. Jändel, M. Sahrling, *Ap. J.* **393** (1992).